Resonant inelastic x-ray scattering and photoemission measurement of O_2: Direct evidence for dependence of Rydberg-valence mixing on vibrational states in O 1s → Rydberg states

T. Gejo, , M. Oura, , T. Tokushima, , Y. Horikawa, , H. Arai, , S. Shin, , V. Kimberg, and , and N. Kosugi

Citation: The Journal of Chemical Physics **147**, 044310 (2017); doi: 10.1063/1.4994895
View online: http://dx.doi.org/10.1063/1.4994895
View Table of Contents: http://aip.scitation.org/toc/jcp/147/4
Published by the American Institute of Physics

Resonant inelastic x-ray scattering and photoemission measurement of O_2: Direct evidence for dependence of Rydberg-valence mixing on vibrational states in O 1s → Rydberg states

T. Gejo,[1,2,a)] M. Oura,[2] T. Tokushima,[2] Y. Horikawa,[2] H. Arai,[2] S. Shin,[2,3] V. Kimberg,[4] and N. Kosugi[5]

[1]*University of Hyogo, Koto 3-2-1, Kamigori-cho 678-1297, Japan*
[2]*Riken SPring-8 Center, Koto 1-1-1, Sayo-cho 679-5148, Japan*
[3]*Institute for Solid State Physics (ISSP), University of Tokyo, Kashiwanoha, Kashiwa, Chiba 277-8581, Japan*
[4]*Royal Institute of Technology, 106 91 Stockholm, Sweden*
[5]*Institute for Molecular Science, Okazaki 444-8585, Japan*

(Received 24 March 2017; accepted 8 July 2017; published online 28 July 2017)

High-resolution resonant inelastic x-ray scattering (RIXS) and low-energy photoemission spectra of oxygen molecules have been measured for investigating the electronic structure of Rydberg states in the O 1*s* → σ* energy region. The electronic characteristics of each Rydberg state have been successfully observed, and new assignments are made for several states. The RIXS spectra clearly show that vibrational excitation is very sensitive to the electronic characteristics because of Rydberg-valence mixing and vibronic coupling in O_2. This observation constitutes direct experimental evidence that the Rydberg-valence mixing characteristic depends on the vibrational excitation near the avoided crossing of potential surfaces. We also measured the photoemission spectra of metastable oxygen atoms (O*) from O_2 excited to 1*s* → Rydberg states. The broadening of the 4*p* Rydberg states of O* has been found with isotropic behavior, implying that excited oxygen molecules undergo dissociation with a lifetime of the order of 10 fs in 1*s* → Rydberg states. *Published by AIP Publishing.* [http://dx.doi.org/10.1063/1.4994895]

I. INTRODUCTION

The O 1s absorption spectra of oxygen molecules have been a subject of great interest for many years owing to the presence of complicated electronic structures.[1–7] Beside a distinct π^* resonance peak that exists at around 531 eV and toward the ionization threshold, the O 1s absorption spectra show unusual complicated structures because O_2 is an open-shell molecule with several dissociative and bound states near the K-edge. Figure 1 shows the total ion yield spectrum of O_2 in the O 1s ionization threshold region.

Below the 1s threshold energy, σ^* resonances and many Rydberg states converging to the two core hole states have been observed, where there are one broad peak with a fine structure and many sharp peaks. The origin of these features had been a topic of debate. Kosugi and co-workers showed that two σ^* excited states are present and that they affect these resonance structures.[1,2] The two σ^* excited states can be characterized as $\sigma^*_u[Q_g]$ [one can also denote as $1s\sigma_g^{-1}(^4\Sigma_g^-)\sigma^*_u(^3\Sigma_u^-)$] and $\sigma^*_u[D_g]$ [$1s\sigma_g^{-1}(^2\Sigma_g^-)\sigma^*_u(^3\Sigma_u^-)$] depending on their convergence to the $^4\Sigma_{g,u}^-$ (quartet) and $^2\Sigma_{g,u}^-$ (doublet) states, respectively, where Q and D denote a quartet and a doublet ion core. The lower ionization energy related to the ion core $^4\Sigma_{g,u}^-$ is 543.39 eV, and the higher one related to $^2\Sigma_{g,u}^-$ is 544.43 eV.[3] It should be noted that $\sigma^*_u[D_g]$ has lower energy than $\sigma^*_u[Q_g]$ because of strong exchange interaction.[2] Therefore, the energy inversion of quartet and doublet states occurs between σ^* and ionic states. The interactions of Rydberg electronic configurations with excited valence configurations due to the vibronic coupling have a large influence on the molecular electronic structure and it is called Rydberg-valence (RV) mixing. Therefore, most of the fine structures are due to Rydberg transition converging to the two ionization thresholds because of RV mixing. Since the $np\sigma_u[Q_g]$ Rydberg state and repulsive $\sigma_u^*[Q_g]$ state can be heavily mixed and can perturb each other via avoided potential-curve crossing, $p\sigma$-type Rydberg transitions have relatively intense structures.

These states have been investigated by high-resolution angle-resolved photo-ion yield spectroscopy (ARPIS) data[1,2] in combination with *ab initio* calculations. Tanaka and co-workers attempted to reassign these states with the help of resonant Auger spectra, which were considered as Auger spectra shifted by the screening energy for a given Rydberg state.[3] Their result was not significantly different from the calculation by Yagishita *et al.*[2] Feifel *et al.*[4,5] and Velkov *et al.*[6] theoretically investigated the origin of these features. Through *ab initio* calculation[4] and wave-packet simulation,[6] they explained that the peaks mainly originate from the drop of the intensity of σ^* peaks due to the crossing of two potential surfaces: that of the 3*p* Rydberg state and of the repulsive σ^* state. Based on this model, Velkov *et al.* successfully explained the long-tailed feature of the σ^* state in the lower-energy region in Fig. 1, together with the intensive $3s\sigma$ feature and the sudden drop of intensity in the nearby higher-energy region. Recently,

a)gejo@sci.u-hyogo.ac.jp

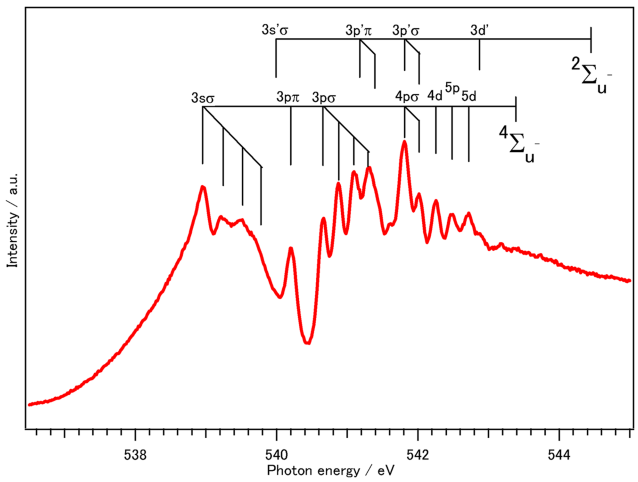

FIG. 1. Total ion yield spectrum of O $1s \rightarrow \sigma_u^*$ resonance of the oxygen molecule. The assignments are based on Ref. 3.

Püttner and Ueda reanalyzed the data of the ARPIS spectra of O_2 below the O 1s ionization threshold by using a sophisticated fit approach.[7] They showed that σ^* resonance shows a narrower peak due to the interaction between σ^* and $3p\sigma$. In accordance with these experimental results, we will discuss, based on an adiabatic model, that the peaks consist of one strong σ^* resonance around 539 eV and many Rydberg states toward the ionization threshold.

Such a complicated electronic characteristic is very difficult to establish comprehensively through experiments involving only ARPIS[1,2,7] or Auger electron spectroscopy.[3] However, energy-tuned x-ray fluorescence spectroscopy, the so-called resonant inelastic x-ray scattering (RIXS) spectroscopy, is a very useful tool for the determination of electronic characteristics in this case[8,9] because the dipole characteristics of the absorption and emission are limited by simple selection rules. In addition, the transition moments between Rydberg and valence orbitals are usually weak compared to those between orbitals with the same characteristics. Thus, RIXS spectroscopy is a useful and sensitive tool to determine the electronic characteristics of complicated electronic and vibronic structures. This is true in the vicinity of the O $1s \rightarrow \sigma^*$ resonance, where RV mixing is present. Recently, we studied the RV mixing in O_2 by the RIXS technique,[10] where the excitations to valence and/or Rydberg orbitals were analyzed by filtering pure valence and pure Rydberg final states.

The autoionization spectra arising from the metastable fragments from 1s → Rydberg states are also helpful. Recently, we studied the low-energy electron spectra of H_2O in the vicinity of the O 1s ionization threshold. The formation of neutral oxygen Rydberg atoms (O*) was observed, and the initially excited electron in a Rydberg orbital was shown to remain associated with O* even after the cleavages of bonds.[11,12] Therefore, the measurement of low-energy electron spectra provides useful information regarding the dynamics of these states. In particular, the Doppler profiles in the autoionization spectra of O* contain information about the kinetics of the dissociation of O_2 in the inner-shell excited state.

In this work, we first show the versatility of the RIXS method by demonstrating the assignment of Rydberg and RV mixing states of O_2 at photon energies across $1s \rightarrow \sigma^*$ resonances. Then, we show using RIXS spectra that, in the σ^* resonance, vibrational excitation is very sensitive to the electronic characteristics because of RV mixing. We also show the experimentally obtained low-energy autoionization spectra of O* from O_2 in the inner-shell excited state. The broadening of the $2s^2 2p^3(^2\mathrm{D})4p$ state of O* has been found with isotropic behavior. This observation can be explained by the short lifetime of the oxygen molecule, which undergoes the dissociation with a lifetime of the order of 10 fs.

II. APPARATUS AND EXPERIMENTAL METHOD

We have previously reported the experimental setup.[13] Briefly, the experiments were performed on the a-branch of the soft x-ray undulator beamline BL17SU at SPring-8. This beamline can provide highly stabilized monochromatic soft x-rays from 300 to 1800 eV with a resolving power of over 10 000.[14,15] The direction of the polarization vector of the incident beam can be switched by changing the operational mode of the undulator. In the present study, we have set the operational mode to be a helical mode in which the degree of circular polarization Pc is approximately 0.98 at 530 eV to achieve a high photon flux.

The energy of the incident photon beam was calibrated by recording the total ion yield spectra of O_2 molecules in the inner-shell excitation region, and the absolute energy scale was established using the data from a previous paper.[3] The accuracy of the energy scale for the incident photon beam was estimated to be approximately ±40 meV. The energy resolution was set to approximately 65 meV at a photon energy of 530 eV to achieve a high photon flux.

The RIXS spectra were recorded using a high-performance slitless spectrometer equipped with a compact flange-mounted liquid flow cell.[16,17] Although this spectrometer was originally developed for studying liquid targets, in the present study, we introduced oxygen gas into the flow cell. This flow cell utilizes a 150-nm-thick Au-coated SiC membrane window to separate the flowing gas at atmospheric pressure from the high vacuum. The spectrometer was calibrated by measuring the normal fluorescence emitted from the core-ionized oxygen molecules and the photons elastically scattered from the target gas. The estimated energy resolution of the spectrometer was 258 meV.

To record the electron kinetic energy spectra, we used a hemispherical electron energy analyzer (VG-Scienta2002) equipped with a gas cell. The lens axis of the analyzer was fixed in the horizontal direction, and the electron analyzer was energy-calibrated by recording a low-energy electron spectrum corresponding to that of O_2 in the vicinity of the 1s ionization threshold.[18] The resolution of the electron analyzer was set to approximately 8 meV, and the typical pressure in the main chamber housing the gas cell was approximately 1.0×10^{-3} Pa during the measurements. The direction of the polarization vector can be switched to vertical or horizontal, and the photons have a polarization degree of 0.90 in this energy region.

III. RESULTS AND DISCUSSION

The ground state of the oxygen molecule has an electronic structure of $^3\Sigma_g^-$:$1\sigma_g^2 1\sigma_u^2 2\sigma_g^2 2\sigma_u^2 3\sigma_g^2 1\pi_u^4 1\pi_g^2 \sigma_u^{*0}$. The dipole character of absorption and emission leads to simple selection rules. The parity selection rule connects initial, excited, and final states after emission either as ungerade–gerade–ungerade (*u*-*g*-*u*) or as gerade–ungerade–gerade (*g*-*u*-*g*) states. Therefore, whenever inner-shell electrons are excited to Rydberg and valence states, excited states should show symmetrical *u*-character as a whole and be in the triplet state, and final states after emission should show symmetrical *g*-character as a whole and also be in the triplet state. The main dipole-allowed final states with high transition moment are $3p\pi_u[A^2\Pi_u]$, $3p\pi_u[a^4\Pi_u]$, $3s\sigma_g[b^4\Sigma_g^-]$, $3p\sigma_u[a^4\Pi_u]$, $\sigma_u{*}[A^2\Pi_u]$, and $\sigma_u{*}[a^4\Pi_u]$, which we denote as $2^3\Sigma_g^-$, $3^3\Sigma_g^-$, $4^3\Sigma_g^-$, $2^3\Pi_g$, $3^3\Pi_g$, and $4^3\Pi_g$, respectively.[10] The dipole transitions between Rydberg and valence orbitals are usually small. Therefore, $2^3\Sigma_g^-$, $3^3\Sigma_g^-$, $4^3\Sigma_g^-$, and $2^3\Pi_g$ Rydberg states are dominant in the RIXS spectra when the 1*s* electron is excited to Rydberg states, whereas $3^3\Pi_g$ and $4^3\Pi_g$ valence states are strongly observed when excited to $\sigma_u{*}$ states.[10] The main ionized states are $X^2\Pi_g$, $a^4\Pi_u$, $A^2\Pi_u$, $b^4\Pi_g^-$, $B^2\Sigma_g^-$, and $c^4\Sigma_u^-$.[10]

As shown in Fig. 1, the lower-energy resonance peak consists of $\sigma_u{*}[D_g]$, $3s\sigma_g[D_u]$, and $3p\pi_u[Q_g]$ states, where Q and D denote the quartet and doublet ion cores. The higher-energy peaks mainly consist of the $3p\sigma_u[Q_g]$ and $4p\sigma_u[Q_g]$ Rydberg states. In the Rydberg states, the DQ interchannel coupling among $[Q_g]$, $[Q_u]$, $[D_g]$, and $[D_u]$ is quite small, although the $3p\sigma_u[Q_g]$ Rydberg state is strongly mixed with the $\sigma_u{*}[Q_g]$ state having DQ interchannel coupling with $\sigma_u{*}[D_g]$ in the Frank-Condon region.[6] The $3p\sigma_u[Q_g]$ vibrational structure up to v = 4 has been observed, although peaks of v = 3, 4 overlap with the $3p\pi_u[D_g]$ state. Here, we discuss $3s\sigma_g[Q_u]$, $ns\sigma_g[Q_g]$, the vibrational structure of $3p\sigma_u[Q_g]$ up to v = 2, and $np\sigma_u[Q_g]$.

A. RIXS spectrum of $3s\sigma_g[Q_u]$ state

In Fig. 1, one can observe a few structures between 539 and 540 eV. Tanaka *et al.*[3] suggested that this structure arises from the vibrational progressions of $3s\sigma_g[Q_u]$. However, the peak at $h\nu_{in} = 539.0$ eV (v = 0) is distinctively strong, while the intensity suddenly drops with increasing photon energy and shows a weak feature. Velkov *et al.* explained that this is due to the decrease in the transition dipole moment near the crossing point between the repulsive σ^* and Rydberg $3s\sigma_g$ potential surfaces.[6]

We have observed the RIXS spectra at the $3s\sigma_g[Q_u]$ Rydberg state and the weak structure nearby. Excitation photon energies and the obtained RIXS spectra are shown in Fig. 2. Two different types of spectra are observed depending on the excitation energy, which indicates that the characteristics of the electronic states are different for different excited states. The central feature at approximately $h\nu_{out} = 525.4$ eV in Fig. 2 is formed by transitions to the $4^3\Pi_g$ ($\sigma_u{*}[a^4\Pi_u]$) valence state.[10] This implies that the $\sigma_u{*}[Q_g]$ orbital is mainly excited, and the transition dipole moments from Q_g to the final states of $a^4\Pi_u$ state are dominant.[10] The intensity of this peak decreases when

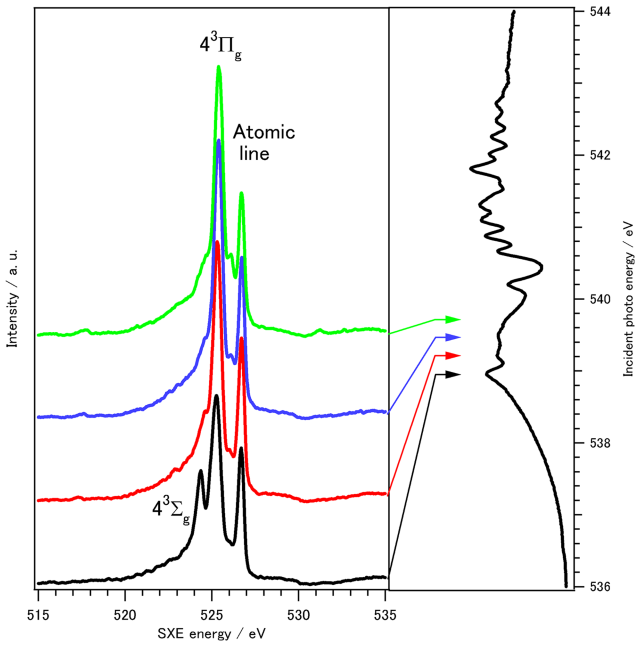

FIG. 2. Experimental RIXS profiles. The excitation energies are shown by the arrows on the x-ray absorption spectrum (inset). These excitation energies correspond to the region of $3s\sigma_g[Q_u]$ Rydberg states.

the photon energy is close to the maximum of resonance. At $h\nu_{in} = 539.01$ eV, the maximum of the σ^* resonance, one can observe a small peak at $h\nu_{out} = 524.4$ eV. This peak has been assigned as the $4^3\Sigma_g^-$ Rydberg state ($3s\sigma_g[b^4\Sigma_g^-]$), which naturally indicates that the peak at $h\nu_{in} = 539.01$ eV in Fig. 2 has a Rydberg character. As shown in Fig. 2, this $4^3\Sigma_g^-$ state vanishes in the shoulder of the next peak when excited at the structure nearby, which implies that this structure has little transition probability to $3s\sigma_g$ at this excitation energy region. This suggests that this state has a slight Rydberg character. This is consistent with the fitting result obtained by Püttner and Ueda,[7] in which the intensity of the peaks in the vibrational excited state is considerably small compared with the vibrational ground state.

From the above observations, this structure can be interpreted as follows. Since the equilibrium geometries of the ground and $3s\sigma_g[Q_u]$ states are very close (~1.2 A), the Franck-Condon factor of the vibrational excited state is very small. As excitation energy increases, $\sigma_u{*}[Q_g]$ valence characteristics dominate. Thus, at excitation photon energies of 539.29 eV, 539.56 eV, and 539.72 eV, the RIXS spectra show slight characteristics of a Rydberg state. Consequently, the vibrational excited states in the absorption spectrum show only a weak structure, and valence characteristics are dominant.

An additional peak at $h\nu_{out} = 526.7$ eV has been observed in Fig. 2. We ascribe this peak to the atomic line $O^*(1s2s2p^5\ ^3P) \rightarrow O^*(1s^2 2s2p^4\ ^3P)$ after ultrafast dissociation caused by the σ^* repulsive potential.[10] We should note that this peak has been observed along the σ^* resonance peak, while on higher-energy Rydberg states, no peak at $h\nu_{out} = 526.7$ eV has been observed. This implies that ultrafast dissociation occurs only at the σ^* resonance peak, which is consistent with the results obtained by Guillemin *et al.*[18] The reason for this is the stronger Rydberg character of the progression of the

$np\sigma_u[Q_g]$ Rydberg state. This Rydberg state is strongly bound, which results in the suppression of the ultrafast dissociative dynamics inherent in the case of the σ^* resonance. A similar phenomenon was observed by Hjelte *et al.*, who investigated atomic Auger lines resulting from fast dissociation only on the σ^* resonance.[19]

B. RIXS spectra of $3s\sigma_g[Q_u]$, $4s\sigma_g[Q_u]$, and $5s\sigma_g[Q_u]$ states

In the absorption spectrum in Fig. 1, no peak has been assigned as $4s\sigma$ and $5s\sigma$.[3] As shown in Fig. 2, the small peak at $h\nu_{out} = 524.4$ eV in the RIXS spectrum can be recognized as a fingerprint of $ns\sigma_g[Q_u]$ Rydberg states because the bands arising from these Rydberg states are expected to be observed in the vicinity of the $4^3\Sigma_g^-$ band ($3s\sigma_g[X^2\Pi_g]$) when excited to $ns\sigma_g[Q_u]$ Rydberg states as the $ns\sigma_g[X^2\Pi_g]$ band. Since the emission photon energy mainly arises from the $[Q_u] \rightarrow [X^2\Pi_g]$ pure valence transition, the $ns\sigma_g[X^2\Pi_g]$ Rydberg peaks in the RIXS spectra should be located almost at the same position.[9]

Figure 3 shows the RIXS spectra excited at $h\nu_{in} = 541.32$ and $h\nu_{in} = 542.02$ eV, together with the RIXS spectrum of the $3s\sigma_g[Q_u]$ state at an excitation photon energy of 539.01 eV. These RIXS spectra clearly show the same peak at the vicinity of $h\nu_{out} = 524.4$ eV, corresponding to $ns\sigma_g[X^2\Pi_g]$ Rydberg states. Therefore, three excited states have $s\sigma_g$-type Rydberg contribution. These peaks have term values of 4.38 eV, 2.07 eV, and 1.37 eV, which correspond to the $3s\sigma_g[Q_u]$ ($\delta = 1.23$), $4s\sigma_g[Q_u]$ ($\delta = 1.43$), and $5s\sigma_g[Q_u]$ ($\delta = 1.84$) states, respectively. Tanaka *et al.* assigned these bands as $3s\sigma_g$, $3p\sigma_u$ $v = 3$, and $4p\sigma_u$ $v = 1$, respectively. Indeed, in the RIXS spectrum at a photon energy of $h\nu_{in} = 541.32$ eV, two strong peaks at $h\nu_{out} = 525.9$ eV and 527.3 eV have been observed. These two peaks have been observed in the vibrational excited state of $3p\sigma_u[Q_g]$, as we will show in Sec. III C. Therefore, the peak at the excitation energy of 541.32 eV also includes the vibrational excited state of $3p\sigma_u[Q_g]$ Rydberg peaks. We have assigned $h\nu_{in} = 541.32$ eV peak as an overlap with $4s\sigma_g[Q_u]$ and $v = 3$ of the $3p\sigma_u[Q_g]$ state. $5s\sigma_g[Q_u]$ states have a relatively large term value. Therefore, we assume that the maximum of this peak is not the precise energy positions of $5s\sigma_g[Q_u]$ because of the overlapping of the other state, and the term values of $5s\sigma_g[Q_u]$ may be smaller than 1.37 eV. The RIXS spectrum at a photon energy of $h\nu_{in} = 542.02$ eV shows a strong $2^3\Pi_g$ (or $np\sigma_u[X^2\Pi_g]$) peak probably arising from the vibrational excited state of $4p\sigma_u$. Therefore, this peak can be assigned as the overlap of $4p\sigma_u[Q_g]$ $v = 1$ and $5s\sigma_g[Q_u]$.

C. RIXS spectrum of $3p\sigma_u^*[Q_g]$

The most interesting point of our spectra is the clear vibrational dependence of RIXS spectra. Figure 4 shows the RIXS spectra for the excitation of $v = 0$, $v = 1$, and $v = 2$ in the $3p\sigma_u^*[Q_g]$ state. The ARPIS spectrum of O_2 shows that the peaks arising from $v = 0$, $v = 1$, and $v = 2$ in the $3p\sigma$ state have no overlaps with other Rydberg states.[2,3,7] As the excitation energy increases, the RIXS spectra drastically change from a distinct strong peak at $h\nu_{out} = 526.5$ eV to the splitting of the peak. The lower-energy side peak is ascribed to $4^3\Pi_g$ ($\sigma_u^*[A^2\Pi_u]$) states, whereas the strong central peak can be assigned as the $2^3\Pi_g$ ($3p\sigma_u[a^4\Pi_u, A^2\Pi_u]$) state.[10]

This splitting is explained by the vibrational-state dependence of RV mixing: at $v = 0$, the $3p\sigma_u[Q_g]$ and $\sigma_u*[Q_g]$ states are weakly mixed. As a result of this weak RV mixing, this state has a strong Rydberg character. Therefore, the strong electronic transition probability to the $2^3\Pi_g$ ($3p\sigma_u[a^4\Pi_u, A^2\Pi_u]$) state is dominant in this $v = 0$ state. As the excitation photon energy increases, the valence character becomes stronger owing to RV mixing because the core-excited valence σ_u^* state interacts non-adiabatically with the $3p\sigma_u$ Rydberg state near the Frank-Condon region ($R \sim 1.2$ Å).[5] Consequently, the RIXS spectra show strong electronic transition probabilities from $\sigma_u^*[Q_g]$ to $\sigma_u^*[a^4\Pi_u]$ valence states. Indeed, in Fig. 3, the intensity of the peak due to the transition to $4^3\Pi_g(\sigma_u^*[a^4\Pi_u])$ increases as the excitation energy increases. Therefore, this drastic change can be elucidated by the difference in degree of RV mixing, i.e., the drastic change of

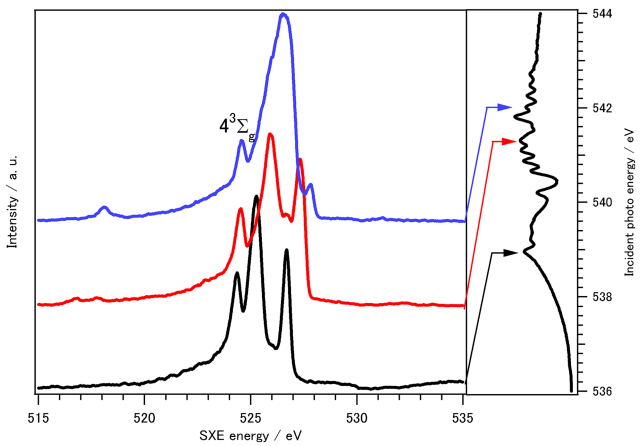

FIG. 3. Experimental RIXS profiles. The excitation energies are shown by the arrows on the x-ray absorption spectrum (inset). These excitation energies correspond to $ns\sigma_g[Q_u]$ Rydberg states.

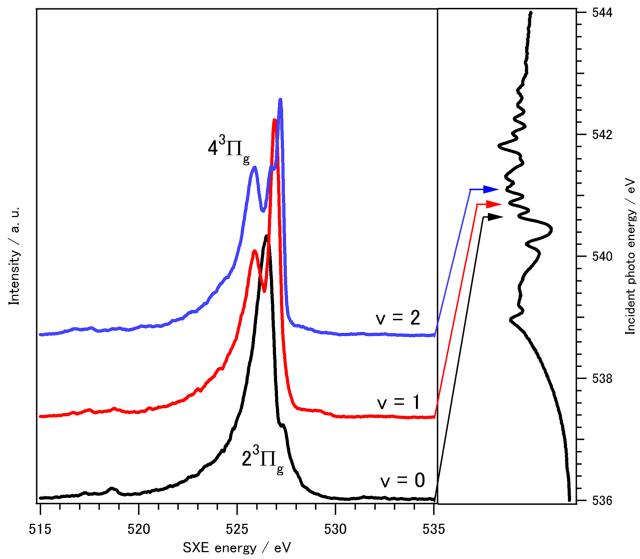

FIG. 4. Experimental RIXS profiles. The excitation energies are shown by the arrows on the x-ray absorption spectrum (inset). These excitation energies correspond to the vibrational state $v = 0$, 1, 2 of the $3p\sigma_u[Q_g]$ Rydberg state.

electronic characteristic from $p\sigma$-type Rydberg to σ^* valence characteristics. Such vibrational dependence on electronic characteristics has been observed by ARPIS spectra in C $1s \rightarrow$ Rydberg excitation of CO_2, where the π^* characteristic is mixed as the bending mode is excited.[20] Since RIXS spectra show the characteristics of electronic states more clearly, they give more direct and stronger evidence compared to ARPIS. Note that the strong peak at $h\nu_{out} = 527$ eV in Fig. 4 may arise from the RV mixing of the $2^3\Pi_g$ and $1^3\Pi_g$ final states with the avoided crossing at ~1.15 Å,[10,21] which can play an additional role in the formation of the RIXS spectra.

D. RIXS spectra of $3p\sigma_u[Q_g]$, $4p\sigma_u[Q_g]$, and $5p\sigma_u[Q_g]$ states

The RIXS technique can be applied to the $np\sigma$ Rydberg series. The RIXS spectrum at $3p\sigma_u[Q_g]$ peaks at $h\nu_{in} = 540.67$ eV shows a distinct, strong peak at $h\nu_{out} = 526.5$ eV. This peak arises from the transition of dipole moments to the $2^3\Pi_g(3p\sigma_u[a^4\Pi_u])$ Rydberg states. We have investigated other Rydberg peaks, which show a strong, distinct single peak at $h\nu_{out} = 526.5$ eV. Since the emission photon energy mainly arises from the $[Q_u]$ to $[a^4\Pi_u]$ valence transition, the $np\sigma_u[a^4\Pi_u, A^2\Pi_u]$ peaks of the RIXS spectra are expected to be located almost at the same position. Figure 5 shows the RIXS spectra at excitation energies of 540.67 eV, 541.81 eV, and 542.26 eV, together with 542.46 eV, 542.72 eV, and 549.56 eV. The first three spectra are very similar, with a distinct, strong peak precisely at $h\nu_{out} = 526.5$ eV corresponding to $np\sigma_u[a^4\Pi_u, A^2\Pi_u]$ Rydberg states. This implies that these three excited states may have a common Rydberg character. Then we can assign the $h\nu_{in} = 541.81$ eV peak to the $4p\sigma_u[Q_g]$ state. Since $h\nu_{in} = 542.26$ eV, the peak has a term value of 1.13 eV ($\delta = 1.53$ for $5p$), which is considerably large for $5p\sigma_u$. Therefore, one can conclude that the main transition arises from $v = 2$ of the $4p\sigma_u[Q_g]$ state. This is partly consistent with the results of Tanaka *et al.*[3] and Püttner and Ueda,[7] who suggested it as a mixing band of the $4p\sigma_u[Q_g]$ and $3d\sigma_u[Q_g]$ states. In Fig. 5, we also show the RIXS spectra at excitation energies of 542.46 eV and 542.72 eV, where the peaks are assigned as $5p\sigma_u[Q_g]$ and $6p\sigma_u[Q_g]$ by Püttner and Ueda.[7] Although there is a peak shift of 0.2 eV from those excited at $3p\sigma_u[Q_g]$ and $4p\sigma_u[Q_g]$, the shapes of the spectra are similar. Therefore, one may conclude that these peaks arise from $5p\sigma_u[Q_g]$ and $6p\sigma_u[Q_g]$ as Püttner and Ueda suggested.[7] However, as the excitation energy becomes close to the ionization threshold, the RIXS spectra become similar to the spectrum in the direct ionization region, which we have shown as the RIXS spectrum excited at $h\nu_{in} = 549.56$ eV in Fig. 5. This implies that, toward the ionization limit, using the RIXS spectra to recognize different electronic states is relatively difficult.

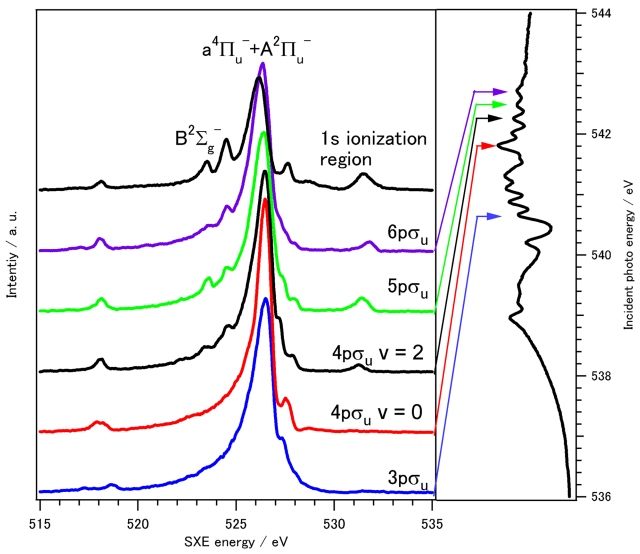

FIG. 5. Experimental RIXS profiles. The excitation energies are shown with the arrows on the x-ray absorption spectrum (inset). These excitation energies correspond to the vicinity of $np\sigma_u[Q_g]$ Rydberg states. The assignments are based on the discussion in the text.

E. The autoionization spectra of σ_*, $3p\sigma_u[Q_g]$ and $4p\sigma_u[Q_g]$ states

In the RIXS spectra, we observed the atomic line at $h\nu_{out} = 526.7$ eV, that is, the $O^*(1s2s2p^5\ ^3P) \rightarrow O^*(1s^22s2p^4\ ^3P)$ transition takes place after ultrafast dissociation only on σ^* resonance. To investigate the dynamics of Rydberg states, we measured the electron spectra of O^* $(2s^22p^3(^2D)nl)$ around this excitation energy region. These O^* states are autoionizing states because they are Rydberg states built on an $O^+(^2D)$ ionic core lying above the $O^+(^4S)$ ionization limit.[23] It has been shown that the initially excited electron in a Rydberg orbital remains with O^* even after the cleavages of bonds.[12,22,24] Figure 6 shows the photoelectron spectra of O_2 obtained at photoexcitation energies of $h\nu_{in} = 538.96$ eV $(3s\sigma_g[Q_u])$, $h\nu_{in} = 540.70$ eV $(3p\sigma_u[Q_g],$

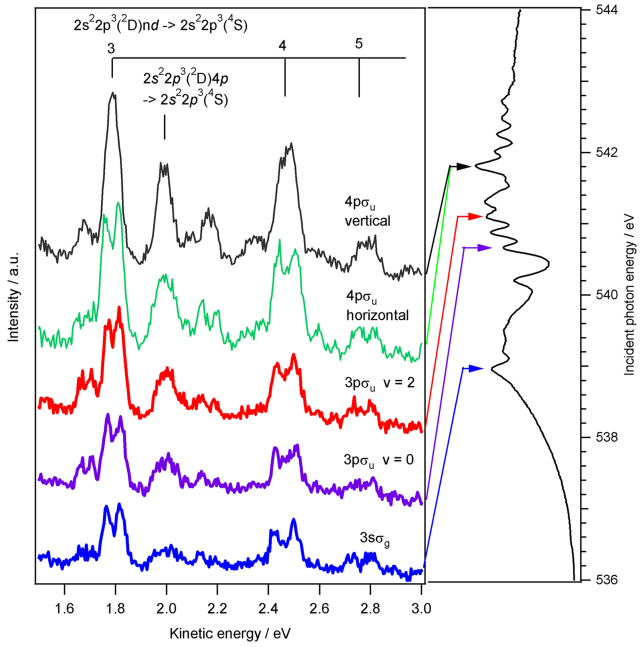

FIG. 6. Photoelectron spectra of O_2 obtained at photoexcitation energies of 538.96 eV $(3s\sigma_g[Q_u])$, 540.67 eV $(3p\sigma_u\ v = 0)$, 541.10 eV $(3p\sigma_u\ v = 2)$, and 541.81 eV $(4p\sigma_u)$. The direction of polarization was chosen as either 0° (horizontal) or 90° (vertical) with respect to the optic axis of the analyzer. All spectra except that denoted as "$4p\sigma_u$ vertical" were measured with the polarization fixed in the horizontal direction.

v = 0), $h\nu_{in}$ = 541.13 eV ($3p\sigma_u[Q_g]$, v = 2), and $h\nu_{in}$ = 541.81 eV ($4p\sigma_u[Q_g]$). The direction of the photon polarization was chosen as either 0° (horizontal) or 90° (vertical) with respect to the optic axis of the analyzer, and except for the spectrum of the $4p\sigma_u$ vertical direction, the spectra were measured with the polarization fixed in the horizontal direction.

We have assigned these lines to the autoionization decay of the O* atom.[18] For example, the strong line at 1.8 eV is due to electrons ejected from the $2s^22p^3(^2D)3d$ excited state of the oxygen atom when the electronic state of the ion core changes from $2s^22p^3(^2D)$ to $2s^22p^3(^4S)$.[25] Other lines can be assigned to the *nd* (*n* = 4, 5) Rydberg series of O*, the transitions of which are also from the core-ionized $2s^22p^3(^2D)$ state to the $2s^22p^3(^4S)$ state; the transition energy between the $2s^22p^3(^2P)$ and $2s^22p^3(^4S)$ states is 3.325 eV.[25] The presence of O* due to the electrons ejected from the $2s^22p^3(^2D)4p$ excited state of the oxygen atom is also observed at 2.0 eV. When $4p\sigma_u[Q_g]$ was excited, the $2s^22p^3(^2D)4p$ state shows stronger intensity. This is mainly due to the 4*p* Rydberg excitations because an initially excited electron in a Rydberg orbital tends to remain in the similar orbital even after the cleavage of the bond.[12]

We should mention that $2s^22p^3(^2D)4p$ states do not show Doppler splitting. In contrast, the other peaks clearly show Doppler splitting, implying that O* atoms are preferentially ejected in the polarization direction and along the analyzer's optic axis. Therefore, the generation of O* in $2s^22p^3(^2D)4p$ states must be insufficient to be observed clearly before dissociation. Note that other mechanisms are conceivable with regard to the generation of the isotropic emission line. For example, a longer lifetime of O_2 in the excited state generates an isotropic emission line. An isotropic one can also be observed if O* in the $2s^22p^3(^2D)4p$ Rydberg state arises from both Σ channel (O* are generated parallel to the polarization direction) and Π channel (O* are generated vertical). However, since O* in the $2s^22p^3(^2D)nd$ Rydberg state shows a high propensity for parallel dissociation, it is very difficult to conclude that only O* in the $2s^22p^3(^2D)4p$ Rydberg state has other dissociation dynamics. The only conceivable reason is the photoemission energy of O* itself that has been influenced and broadened.

If the lifetime is indeed shorter than the dissociation time, the observation of $2s^22p^3(^2D)np$ states with no Doppler splitting can be attributed to the broadening due to the perturbation of the counterpart of the O atom or the O^+ ion before the completion of dissociation. This can be rationalized by the fact that, in H_2O where relatively long lifetime can be expected, no $2s^22p^3(^2D)np$ state has been observed after inner-shell excitation.[12] The application of an atomic orbital calculation program (COWAN code)[26] suggested that the lifetime of the $2s^22p^3(^2D)4p$ state of O* is 9.6 fs and its peak should be located at 1.95 eV in the photoelectron spectra; furthermore, the lifetime of the $2s^22p^3(^2D)3d$ state is 3.7 ns and should be located at 1.63 eV.

As we have mentioned in Sec. III A, the ultrafast dissociation occurs only at the σ* resonance peak, not at Rydberg peaks including $3p\sigma_u[Q_g]$ and $4p\sigma_u[Q_g]$ states. Therefore, assuming that the lifetime of the ultrafast dissociation is of the order of fs, we can deduce that the lifetime of oxygen molecules in the $3p\sigma_u[Q_g]$ and $4p\sigma_u[Q_g]$ states has a lifetime greater than fs. If we, again, consider that the lifetime of the $2s^22p^3(^2D)4p$ state of O* is 9.6 fs, the dissociation time after resonant Auger decay must be close to 9.6 fs to be observed. Since the resonant Auger decay is a fast process (~a few fs), we can say that the oxygen molecules excited to the $3p\sigma_u[Q_g]$ and $4p\sigma_u[Q_g]$ Rydberg states undergo the dissociation with a lifetime of the order of 10 fs.

IV. SUMMARY

RIXS spectra of oxygen molecules have been measured for investigating the electronic structure of RV mixing of the σ* state in the K-edge region. We have successfully made new assignments of several Rydberg states. The RIXS spectra show clear evidence that the bond length is very sensitive to the electronic character because of RV mixing. This technique can be useful for the assignment of peaks in other molecules such as NO_2 and NO, which show complicated structures due to the existence of singlet and triplet states.

The photoemission spectra in the low-energy region arising from O* photoemission may prove to be a unique experimental technique as an internal clock: since O* in the Rydberg state has a given lifetime, the spectral broadening (O_2 case) and vanishing (H_2O case) can be analyzed with the consideration of its lifetime.

ACKNOWLEDGMENTS

The synchrotron radiation experiments were performed at BL17SU in SPring-8 with the approval of RIKEN (Proposal Nos. 20070113, 20080029, and 20150039). T.G. thanks JSPS for financial support (Grant No. 16K05520). V.K. acknowledges the Knut and Alice Wallenberg foundation (No. 2013.0020) and the Swedish Research Council (No. 2015-04510) for financial support.

[1] N. Kosugi, E. Shigemasa, and A. Yagishita, Chem. Phys. Lett. **190**, 481 (1992).
[2] A. Yagishita, E. Shigemasa, and N. Kosugi, Phys. Rev. Lett. **72**, 3961 (1994).
[3] T. Tanaka, R. Feifel, M. Kitajima, H. Tanaka, S. L. Sorensen, R. Sankari, A. De Fanis, M.-N. Piancastelli, L. Karlsson, and K. Ueda, Phys. Rev. A **78**, 022516 (2008).
[4] R. Feifel, Y. Velkov, V. Carravetta, C. Angeli, R. Cimiraglia, P. Satek, F. Gel'mukhanov, S. L. Sorensen, M.-N. Piancastelli, A. De Fanis, K. Okada, M. Kitajima, T. Tanaka, H. Tanaka, and K. Ueda, J. Chem. Phys. **128**, 064304 (2008).
[5] R. Feifel, T. Tanaka, M. Kitajima, H. Tanaka, A. De Fanis, R. Sankari, L. Karlsson, S. Sorensen, M.-N. Piancastelli, G. Prümper, U. Hergenhahn, and K. Ueda, J. Chem. Phys. **126**, 174304 (2007).
[6] Y. Velkov, V. Kimberg, N. Kosugi, P. Salek, and F. Gel'mukhanov, Chem. Phys. Lett. **476**, 147 (2009).
[7] R. Püttner and K. Ueda, J. Chem. Phys. **145**, 224302 (2016).
[8] F. Hennies, S. Polyutov, I. Minkov, A. Pietzsch, M. Nagasono, H. Ågren, L. Triguero, M.-N. Piancastelli, W. Wurth, F. Gel'mukhanov, and A. Föhlisch, Phys. Rev. A **76**, 032505 (2007).
[9] P. Glans, K. Gunnelin, P. Skytt, J.-H. Guo, N. Wassdahl, J. Nordgren, H. Ågren, F. Kh. Gel'mukhanov, T. Warwick, and E. Rotenberg, Phys. Rev. Lett. **76**, 2448 (1996).
[10] V. Kimberg, T. Gejo, M. Oura, T. Tokushima, Y. Horikawa, H. Arai, and S. Shin, Phys. Rev. A **85**, 032503 (2012).
[11] T. Gejo, M. Oura, M. Kuniwake, K. Honma, and J. R. Harries, J. Phys.: Conf. Ser. **288**, 012023 (2011).
[12] T. Gejo, E. Shigemasa, Y. Hikosaka, O. Takahashi, and K. Honma, J. Chem. Phys. **140**, 214310 (2014).

[13]M. Oura, O. Takahashi, T. Gejo, T. Tokushimal, Y. Horikawa, Y. Senba, H. Ohashi, and S. Shin, J. Phys.: Conf. Ser. **235**, 012016 (2010).
[14]H. Ohashi *et al.*, AIP Conf. Proc. **879**, 523 (2007).
[15]Y. Senba, H. Ohashi, H. Kishimoto, T. Miura, S. Goto, S. Shin, T. Shintake, and T. Ishikawa, AIP Conf. Proc. **879**, 718 (2007).
[16]T. Tokushima, Y. Harada, O. Takahashi, Y. Senba, H. Ohashi, L. G. M. Pettersson, A. Nilsson, and S. Shin, Chem. Phys. Lett. **460**, 387 (2008).
[17]Y. Horikawa, T. Tokushima, Y. Harada, O. Takahashi, A. Chainani, Y. Senba, H. Ohashi, A. Hiraya, and S. Shin, Phys. Chem. Chem. Phys. **11**, 8676 (2009).
[18]R. Guillemin, M. Simon, and E. Shigemasa, Phys. Rev. A **82**, 051401 (2010).
[19]I. Hjelte, O. Björneholm, V. Carravetta, C. Angeli, R. Cimiraglia, K. Wiesner, S. Svensson, and M. N. Piancastelli, J. Chem. Phys. **123**, 064314 (2005).
[20]J. Adachi, N. Kosugi, E. Shigemasa, and A. Yagishita, J. Chem. Phys. **100**, 19783 (1996).
[21]B. R. Lewis, S. T. Gibson, S.S. Banerjee, and H. Lefebvre-Brion, J. Chem. Phys. **113**, 2214 (2000).
[22]E. Melero García, A. Kivimäki, L. G. M. Pettersson, J. Álvarez Ruiz, M. Coreno, M. de Simone, R. Richter, and K. C. Prince, Phys. Rev. Lett. **96**, 063003 (2006).
[23]M. E. Rudd and K. Smith, Phys. Rev. **169**, 79 (1968).
[24]A. Kivimäki, M. Corero, R. Richter, J. Álvarez Ruiz, E. Melero García, M. de Simone, V. Feyer, G. Vall-llosera, and K. C. Prince, J. Phys. B: At., Mol. Opt. Phys. **39**, 1101 (2006).
[25]See http://physics.nist.gov/PhysRefData/ASD/levels_form.html for information about O* energy levels.
[26]R. D. Cowan, *The Theory of Atomic Structure and Spectra* (University of California Press, Berkeley, 1981).